Remote Sensing of Environment 260 (2021) 112438

Contents lists available at ScienceDirect

Remote Sensing of Environment

journal homepage: www.elsevier.com/locate/rse

Performance stability of the MODIS and VIIRS LAI algorithms inferred from analysis of long time series of products

Kai Yan [a,b,c,*], Jiabin Pu [a,*], Taejin Park [d,e], Baodong Xu [b,c], Yelu Zeng [f], Guangjian Yan [c], Marie Weiss [g], Yuri Knyazikhin [b], Ranga B. Myneni [b]

[a] School of Land Science and Techniques, China University of Geosciences, Beijing 100083, China
[b] Department of Earth and Environment, Boston University, Boston, MA 02215, USA
[c] State Key Laboratory of Remote Sensing Science, Jointly Sponsored by Chinese Academy of Sciences and Beijing Normal University, Beijing 100101, China
[d] NASA Ames Research Center, Moffett Field, CA 94035, USA
[e] Bay Area Environmental Research Institute, Moffett Field, CA 94035, USA
[f] Department of Global Ecology, Stanford University, CA 94305, USA
[g] Institut National de la Recherche Agronomique, Université d'Avignon et des Pays du Vaucluse (INRA-UAPV), 228 Route de l'Aérodrome, 84914 Avignon, France

ARTICLE INFO

Editor: Jing M. Chen

Keywords:
Leaf area index (LAI)
Performance stability
Trend detection
Product quality
MODIS
VIIRS

ABSTRACT

The science teams of Moderate Resolution Imaging Spectroradiometer (MODIS) and Visible Infrared Imager Radiometer Suite (VIIRS) have been supporting various global climate, biogeochemistry, and energy flux research efforts by producing valuable long-term Leaf Area Index (LAI) products. Although intensive LAI validation studies have been carried out globally, retrieval accuracy has been assessed only over short time spans and product quality is reported as a constant based on the assumption that it is stationary. However, a preliminary evaluation found a time-dependent signal degradation of the MODIS sensors which may cause the uncertainty of the Bidirectional Reflectance Factor (BRF) product to exceed the preset uncertainty buffer in the retrieval algorithm and result in MODIS LAI quality variation and time-series inconsistency with VIIRS LAI. Therefore, to ensure the reliability of trend-detection studies and to answer the critical question of whether the algorithm configuration is still suitable for the uncertainty level of present BRF product, there is a need for a more comprehensive investigation regarding the performance stability of LAI retrieval algorithm due to model uncertainty and input uncertainties. This paper reports analyses of inter-annual stability and trends of LAI uncertainties (inferred from product quality flag rather than ground-based validation) as well as LAI magnitudes using multi-year (MODIS: 2001–2019, VIIRS: 2013–2019) and multi-site (445 sites) datasets. We found that the quality metrics of the two products are consistent across different biome types and LAI values (R^2 ranged from 0.88 to 0.99). In the 19-year MODIS period, we found a significant increasing trend in LAI magnitudes (4.5%/decade) which agrees with previous reports, while there was no significant trend in product quality. Moreover, quality metrics showed much smaller inter-annual variations than LAI values, which confirms the performance stability of retrieval algorithms and suggests that the configuration of MODIS algorithm is still compatible with the uncertainty of algorithm inputs. Additionally, this study provides support to the "Greening Asia" studies by eliminating the possibility that the "greening" could be attributed to artificial trends caused by sensor degradation. We also found very small inter-annual variations in atmospheric conditions (e.g., cloud and aerosols), which further assures that the performance stability of retrieval algorithm. Overall, our results demonstrate the robustness of the retrieval algorithm in the presence of changes in input uncertainties. The temporal stability of the algorithm performance indirectly strengthen the confidence in the continuous use of MODIS LAI products either independently or in combination with its successor - VIIRS LAI - to study global and regional vegetation dynamics

* Corresponding authors at: School of Land Science and Techniques, China University of Geosciences, Beijing 100083, China.
E-mail addresses: kaiyan@cugb.edu.cn (K. Yan), pujiabin@cugb.edu.cn (J. Pu).

https://doi.org/10.1016/j.rse.2021.112438
Received 19 May 2020; Received in revised form 24 March 2021; Accepted 2 April 2021
Available online 14 April 2021

1. Introduction

Terrestrial vegetation plays an important role in the biosphere, regulating global carbon, water, and energy cycles (Sellers et al., 1997; Zhang et al., 2017). Leaf Area Index (LAI), generally defined as one-sided green leaf area per unit ground horizontal surface area, is an essential variable for characterizing the structure and function of vegetation canopies (Fang et al., 2019; Jacquemoud et al., 1992; Knyazikhin et al., 1998). Representing a milestone in Earth observations, Moderate Resolution Imaging Spectroradiometer (MODIS) observations are used to generate a series of data products, including LAI, and support various studies of global climate, biogeochemistry and energy flux dynamics (Knyazikhin, 1999; Myneni and Park, 2015; Yan et al., 2016a). Inspired by the success of the MODIS sensor, the first Visible Infrared Imager Radiometer Suite (VIIRS) was designed and launched in 2012 to extend this valuable long-term data record (Justice et al., 2013; Park et al., 2017; Yan et al., 2018). Currently, the science teams of these programs have released about 21 years of MODIS (2000 to present) and 9 years of VIIRS (2012 to present) global LAI time-series datasets.

Long-period LAI time-series are essential inputs for land surface models (Lafont et al., 2012; MacBean et al., 2015) and the global dynamic monitoring of terrestrial ecosystems (Hill et al., 2006). MODIS & VIIRS LAI datasets have been widely applied in terrestrial carbon simulation (Kala et al., 2014), monitoring the seasonal and interannual variations in temperate deciduous forests (Tang et al., 2013), and investigating spatial trends in terminal droughts (Chakroun et al., 2014; Dhorde and Patel, 2016; Mariano et al., 2018), among others. The phenomenon of the "Greening Earth", in particular, has attracted intensive studies using MODIS & VIIRS observations. Based on these studies, the global LAI time-series suggests that one-third of the Earth's vegetated area is greening and only 5% is browning (Chen et al., 2019; Zhang et al., 2017; Zhu et al., 2016). These datasets further support studies of the relationship between vegetation dynamics and global climate change or human activities (Chen et al., 2019; Chen and Dirmeyer, 2016; Mao et al., 2013; Zhu et al., 2016).

The validity and conclusions of the above studies depend on the reliability of the LAI products. There have been many studies that have quantified the accuracy of the MODIS & VIIRS LAI datasets, which can be divided into three groups. The first group includes theoretical derivations based on model mechanism and error propagation. The product science team analyzed the uncertainties in the inputs and the basic models and described the theoretical uncertainty for each released version of the MODIS & VIIRS LAI products (Knyazikhin, 1999; Myneni et al., 2002; Park et al., 2017). The theoretical uncertainty for each pixel is stored in Quality Assessment (QA) layers. Based on QA information, Fang et al. conducted a series of MODIS LAI uncertainty studies (Fang et al., 2019; Fang et al., 2013; Fang et al., 2012). The second group dealt with intercomparisons with other products or mutual verifications with other variables. Comparisons among different LAI products at the regional or global scale are commonly used as a low-cost quality assessment method. Intensive efforts have been focused on the consistency between different versions of MODIS & VIIRS LAI (Serbin et al., 2013; Yan et al., 2018; Yan et al., 2016a) and agreement with other global products (Claverie et al., 2013; Fang et al., 2012; Fuster et al., 2020; Liu et al., 2018; Wang and Liang, 2013; Weiss et al., 2014; Yan et al., 2016b). It has been reported that MODIS LAI maintained a good consistency with its previous versions and its successor VIIRS; also, MODIS & VIIRS showed good agreement with other validated products (Xu et al., 2018; Yan et al., 2018). Finally, the third group of LAI evaluation efforts includes direct validations using ground-based LAI measurements. Comparisons with ground LAI observations demonstrated that MODIS LAI performs well both in terms of seasonal trajectories and spatial correlations but underestimates large LAI values (De Kauwe et al., 2011; Yan et al., 2016b). Although the above three evaluation methods have been carried out intensively on MODIS and VIIRS products, their quality (i.e. LAI uncertainty) has been checked only over short time spans and reported as a constant value based on the assumption that they are stationary.

Because both Terra and Aqua MODIS have far exceeded their lifetime design of 6 years (Skakun et al., 2018; Xiong et al., 2016; Xu et al., 2018), the calibration team has observed obvious degradation in the MODIS sensor (Wang et al., 2012; Xiong et al., 2001). However, the effects of sensor degradation are minimized due to improved algorithms and adjustments to atmospheric corrections, as demonstrated in the Bidirectional Reflectance Factors (BRFs) product (Lyapustin et al., 2014). To enhance the robustness of the MODIS LAI retrieval algorithm, not only should the BRFs that are used as input to the retrievals, but also their uncertainties be taken into account by the configuration of the algorithm. The science team defined an uncertainty buffer for the BRFs (Near-Infrared (NIR): 20%, Red: 5%) (Knyazikhin et al., 1998), and it will be reflected in both whether the main algorithm is used and the StdLAI values when the uncertainties of the BRFs used exceed the preset buffer. That is to say, if significant changes are found in theoretical quality metrics (main algorithm retrieval rate (RI) and StdLAI), the science team need to adjust the uncertainty buffer which does not fit with the actual uncertainties of the BRF products. In the meantime, the VIIRS instrument onboard the Suomi National Polar-Orbiting Partnership (S-NPP) and Joint Polar Satellite System (JPSS) was designed on the MODIS heritage and has the goal of ensuring long-term continuity of valuable Earth System Data Records (ESDRs) (Justice et al., 2013). VIIRS LAI products are available from 2012 to present with currently a 9-year overlap period with MODIS, allowing for MODIS-VIIRS joint analyses and usages. In this context, it is essential to examine the performance stability of LAI retrieval algorithm to answer the following three questions: 1) whether the configuration of the LAI retrieval algorithm is still applicable to the uncertainty of current BRF products; 2) whether the performance stability of the LAI retrieval algorithm is sufficient to confirm the published trend-related studies in the context of the MODIS sensor degradation; 3) whether the consistency of LAI values and product quality can support the joint use of MODIS and VIIRS LAIs after the retirement of the MODIS instrument.

This research is based on the assumption that there are trends and significant inter-annual variations in the magnitudes of LAI for long time series, however, the product quality should remain consistent, resulting in more stable quality metrics. Thus, we investigated the above questions in three steps. Firstly, we compared the LAI stability characteristics from the MODIS and VIIRS products over the overlapping period to check their product quality (inferred from product quality flag rather than ground-based validation) consistency. Secondly, we conducted a comprehensive spatio-temporal analysis of inter-annual variations in product quality over the full data periods to assess its stability. Finally, we performed a trend analysis in the MODIS LAI magnitudes and its product quality to revisit the previously published hypothesis "Greening Earth". Note that we exclude VIIRS from this analysis as its operational period is not long enough for a credible trend detection.

The structure of this paper is as follows. Section 2 describes datasets and methodologies for the evaluation of the performance stability of LAI retrieval algorithm. Section 3 details the results about the stability analysis, trend detection, and uncertainty comparison at both site and tile scales, as well at a continental scale to keep a special eye on the "Greening Asia" phenomenon. We discuss the relationship between LAI magnitudes and product qualities and the impact of the atmosphere condition on LAI retrievals in Section 4. Finally, Section 5 provides concluding remarks.

2. Datasets and methodology

2.1. MODIS & VIIRS LAI products

The operational MODIS & VIIRS algorithm includes the main algorithm, which is based on the Radiative Transfer Equation (RTE) and a

backup algorithm, which uses an empirical relationship between the Normalized Difference Vegetation Index (NDVI) and canopy LAI (Myneni et al., 2002; Yan et al., 2018). The algorithm inputs BRFs in the Red and NIR bands, their uncertainties, sun-sensor geometry, and a biome classification map (both MODIS and VIIRS use the same land cover map). The algorithm can be summarized in the following steps. Firstly, the main algorithm parametrizes the variables used in photon transport theory by a biome classification map, each biome type incorporates a structural pattern of vegetation, canopy type, spectral reflectance, and transmittance. Secondly, the canopy reflectance model is constructed by these parameters and is used to evaluate a weight coefficient as a function of sun-sensor geometry, wavelength, and LAI. BRFs are computed from this weight coefficient and the canopy reflectance model. Next the algorithm tests the eligibility of the canopy radiation model to generate a Look-Up-Table (LUT) file. When a given accuracy is met, the given atmospherically corrected BRF is compared to the model BRF stored in biome-specific LUT files and the corresponding LAIs are stored as selected values. Finally, the mean and standard deviation of the selected LAIs are reported as the retrieval and its uncertainty (Knyazikhin, 1999; Knyazikhin et al., 1998). If the main algorithm fails to localize a solution, the empirical backup algorithm is triggered to retrieve LAI.

Performance analyses suggest that the best quality, high-precision retrievals are obtained from the main algorithm (Chen et al., 2019; Yan et al., 2016a; Yang et al., 2006). In the case of dense canopies, the reflectance saturates and becomes weakly sensitive to changes in canopy properties. The reliability of LAIs retrieved under saturated conditions is lower compared to that generated from unsaturated BRFs. Such retrievals are flagged in the algorithm path QA variable indicating the algorithm used (from highest to lowest quality): the main algorithm without saturation, the main algorithm with saturation, the backup algorithm due to sun-sensor geometry, and the backup algorithm due to other reasons. The QA variables also provide information about the cloud state, aerosol loading, and the presence of snow, which are inherited from the upstream BRF product (Knyazikhin, 1999).

In this study, we used the latest Collection 6 MODIS (MOD15A2H, 2001–2019) and Collection 1 VIIRS (VNP15A2H, from 2013 to 2019) LAI products, which are at 500-m spatial and 8-day temporal resolution (Generally, there are 46 composites per year, but due to the influence of the sensor or other factors, one or two composites may be lost). MODIS data for 2000 and VIIRS data for 2012 were excluded because they were incomplete sets (MODIS data have been available since February 18, 2000, and VIIRS data are since January 19, 2012). Data were projected on a sinusoidal grid and distributed as standard Hierarchical Data Format (HDF) files. Each file includes six Science Data Sets (SDSs): Fraction of Photosynthetically Active Radiation absorbed by vegetation (FPAR), LAI, FparLai_QC, FparExtra_QC, FparStdDev, and LaiStdDev. LAI and LaiStdDev layers store the LAI retrieval and its standard deviation. FparLai_QC and FparExtra_QC layers provide information about the algorithm path and atmosphere condition, respectively (Knyazikhin, 1999; Knyazikhin and Myneni, 2018; Myneni and Park, 2015; Park et al., 2017). Therefore, we used these four SDSs for this study.

2.2. MODIS land cover product

The MODIS land cover product (MCD12Q1) is created by classifying spectral-temporal features derived from reflectance data. It maps the global land cover type at 500-m spatial resolution at an annual time step (Sulla-Menashe and Friedl, 2018). Here, we used the LAI legacy classification schemes in which global vegetation is stratified into eight biomes (B1: grasses and cereal crops; B2: shrubs; B3: broadleaf crops; B4: savannas; B5: Evergreen Broadleaf Forests (EBF); B6: Deciduous Broadleaf Forests (DBF); B7: Evergreen Needleleaf Forests (ENF); and B8: Deciduous Needleleaf Forests (DNF)) (Sulla-Menashe and Friedl, 2018; Yan et al., 2016b). Four years (2003, 2008, 2012 and 2017) of MCD12Q1 data were used in this study to control for land cover changes and corresponding effects on LAI magnitude and product quality.

2.3. Study area

The Benchmark Land Multisite Analysis and Intercomparison of Products (BELMANIP) version 2.1 includes 445 sites located in relatively flat and homogeneous areas (Baret et al., 2006). Using BELMANIP sites we not only reduce the volume of computation over the whole globe but also reduce the uncertainty caused by registration bias and land cover misclassification. This is necessary and important since our paper focuses on whether the quality of the LAI product remains stable, which may be caused by sensor degradation or annual atmospheric conditions variation rather than the overall LAI accuracy. The BELMANIP network of sites was originally designed based on the GLC2000 land cover map (Bartholome and Belward, 2005), by investigating the homogeneity of the sites over a 10 by 10 km^2 square area. In this study, we considered a spatial resolution of 500 m and selected the 3 km × 3 km areas centered on the site locations as our study area for each site (see Fig. S1). Thus, each site contains 36 LAI pixels. Fig. S2 shows the biome type distribution in each 3 km × 3 km BELMANIP site based on the land cover product of 2017. These sites are dominated by one biome type with better ground homogeneity which can avoid introducing additional uncertainty (e.g., geometric registration error). It also shows that the percentage of DNF (B8) is very low and we note that DNF and ENF (B7) use the same LUT to produce the MODIS & VIIRS LAI product. Thus, we excluded DNF and focused on the remaining 7 biome types. We selected LAI pixels in these 445 sites that had unchanged land cover type over the four years (2003, 2008, 2012, and 2017); the number of available pixels for each biome type ranged from 578 (B3, broadleaf crops) to 4033 (B1, grasses and cereal crops).

To check the spatial distribution of LAI product quality, we analyzed the variation of the global LAI magnitudes and quality metrics by downscaling method (500 m to 5 km).We also selected 7 single-biome-dominated tiles (2400 × 2400 pixels for each tile) as representative of different biome types: h23v04 (B1), h29v11 (B2), h25v06 (B3), h12v03 (B4), h11v09 (B5), h12v04 (B6), and h20v02 (B7) in order to see the changes in LAI and its quality metrics under a specific biome type. These tiles have the highest percentage of the specific biome (coverage of B1: 84.08%, B2: 97.55%, B3: 33.42%, B4: 73.29%, B5: 94.21%, B6: 33.53%, and B7: 31.53%) over the globe, while we only analyze the pixels in these tiles that correspond to biome types. DBF (B8) was not analyzed because there was no tile where this biome occupied more than 15% of the surface.

We also selected the Asian region since it has undergone significant greening, which has been shown by remote sensing datasets. The studied region ranged from 64.35° E to 139.06° E and from 2.74° N to 58.32° N, covering the whole of China, India, the southern part of Siberia and the northern part of Southeast Asia.

2.4. Product quality metrics and their stability analysis

We used the standard deviation of all LAI candidates (StdLAI in the "LaiStdDev" layer) and the retrieval index (RI in the "FparLai_QC" layer) as the two metrics of LAI product quality. Based on the uncertainty theory embedded in the MODIS & VIIRS retrieval algorithm, the LAI standard deviation of all acceptable solutions in the LUT is reported as the theoretical uncertainty caused by both the input uncertainty (biome type and BRF uncertainty) and model uncertainty (Knyazikhin, 1999; Knyazikhin et al., 1998). This metric is taken as the characteristics of the solution accuracy and has been used for the evaluation of MODIS & VIIRS products by Fang et al. (Fang et al., 2019; Fang et al., 2013). However, StdLAI is only generated when the main algorithm is used and StdLAI is calculated in different ways under saturated and unsaturated conditions (Knyazikhin, 1999; Myneni and Park, 2015). Furthermore, due to the regularization introduced by the algorithm, StdLAI is artificially degraded in the case of large LAI values (Knyazikhin, 1999), so

this metric cannot fully characterize the quality of the product. Therefore, because StdLAI has its limitation as the only criterion for evaluating LAI uncertainty, we also used the Retrieval Index (RI) as an additional product quality metric that characterizes the proportion of the high precision retrievals which have good quality (Xu et al., 2018). The RI (see Eq. (1)) is the percentage of pixels for which the RTE-based main algorithm produces a retrieval and it characterizes the overall quality at a regional scale (Xu et al., 2018; Yan et al., 2018; Yan et al., 2016b). With the retrieval rates of the different algorithmic paths at the regional or global scales, we can evaluate the overall quality of the VIIRS and MODIS products. Therefore, while the StdLAI is the product quality metric for each single pixel, the RI provides the overall evaluation of a certain number of pixels. The reliable analysis of product quality requires a combination of these two metrics.

$$\mathrm{RI} = \frac{\text{N.of pixels retrieved by the main algorithm}}{\text{N.of main algorithm} + \text{N.of back} - \text{up algorithm}} \tag{1}$$

In this paper, the mean value of 46 composites of LAI retrievals over a year for time-series analysis was used. We also used the Standardized Anomaly (SA) to quantify the trend of time-series of both LAI and its product quality metrics to better compare the trends of different variables (Yan et al., 2018). SA was calculated as:

$$\mathrm{SA}(i) = \frac{\mathrm{X}(i) - \mathrm{mean}(\mathrm{X})}{\mathrm{mean}(\mathrm{X})} \tag{2}$$

where X and i are the variable time-series and the time, respectively.

The Mann Kendall (MK) test is a common statistical tool for climate diagnostics and prediction (see Eqs. (3)–(5)) which determines whether there are significant trends in a time-series (Gocic and Trajkovic, 2013). We employed the MK test for all trend analyses to make sure that the detected trend was statistically significant,

$$S = \sum_{i=1}^{n-1} \sum_{j=i+1}^{n} sgn\left(x_j - x_i\right) \tag{3}$$

$$Var(S) = \frac{n(n-1)(2n+5) - \sum_{i=1}^{m} t_i(t_i-1)(2t_i+5)}{18} \tag{4}$$

$$\mathrm{Z_s} = \begin{cases} \dfrac{\mathrm{S}-1}{\sqrt{\mathrm{Var(S)}}}, \text{if S} > 0 \\ 0, \text{if S} = 0 \\ \dfrac{\mathrm{S}+1}{\sqrt{\mathrm{Var(S)}}}, \text{if S} < 0 \end{cases} \tag{5}$$

where S is the sum of the step function values of the difference between the values at any two different points in the time series and n is the number of data, m is the number of tied groups (recurring data sets) in the data, and t_i is the number of the ties (the number of repeats in the extent i). When $|Z_s| > Z_{1-\alpha/2}$, the null hypothesis (i.e., no trend) is rejected and the α is a special significance level. In this paper, we selected $\alpha = 0.05$ and the $Z_{1-\alpha/2} = 1.96$.

Analysis of Variance (ANOVA) is used to access the significant differences in the means between two and more samples. The basic steps of the entire ANOVA are as follows: 1) Set the original hypothesis: H0 - no difference; H1 - a significant difference. 2) Select the test statistic: The test statistic used in ANOVA is the F statistic, which is the ratio of between-group variability to within-group variability. 3) Calculate the observed value of the test statistic and the probability P-value: the purpose of this step is to calculate the observed value of the test statistic and the corresponding probability P-value. 4) Given the significance level, and make a decision. In this paper, when the $P > 0.05$, the hypothesis H0 is accepted.

We used the Coefficient of Variation (CV, see Eq. (6)) as an indicator to analyze the inter-annual variation in LAI and product quality metrics. The CV was used to measure the variability of the annual means for LAI, R1, and StdLAI, independently of the unit and absolute magnitudes of the variables (Abdi, 2010),

$$\mathrm{CV} = \frac{\mathrm{Std(X)}}{\mathrm{mean(X)}} \tag{6}$$

where X is the time-series which is based on the annual averages of LAI, RI, and StdLAI (MODIS: 2001–2019, VIIRS: 2013–2019).

3. Results

3.1. Product quality comparison between MODIS and VIIRS LAI

To check the consistency of MODIS and VIIRS LAI in terms of product quality, we compared the annually averaged values of two selected product quality metrics, RI (Fig. 1) and StdLAI (Fig. S3) in different biome types and LAI magnitudes for the period from 2013 to 2019. We found that overall RI and StdLAI from MODIS and VIIRS are highly consistent, with the coefficient of determination (R^2) of 0.88 for RI (Fig. 1h) and 0.99 for StdLAI (Fig. S3h). VIIRS's shrub class (B2) does not use the main algorithm when the LAI is very high (Fig. 1b). In other words, there are no StdLAI values when LAI is larger than 5.5 (Fig. S3b). MODIS provides a better main algorithm coverage in the case of high LAI values in shrubs (B2) and broadleaf crops (B3) compared to VIIRS (Fig. 1b and c). Although a lower percentage of high LAI for all of these two biome types, this still reflects the imperfect configuration of biome-specific LUT parameters (i.e., single scattering albedo) for VIIRS observations (Yan et al., 2018). For the other 5 biome types, at low LAIs, the RI of MODIS and VIIRS are very close to each other. However, the correlation of RI fluctuates more at high LAIs which could be due to more retrievals under saturated condition (see Fig. 10 and Fig. S6). Fig. 1 also indicates that the dots with high RI all tend to be blue (smaller LAI) except in broadleaf forests (B5 and B6), which means that the algorithm performs better at low LAI values for most biomes. For all biome types, the LAI standard deviations increased first and then decreased with increasing LAI (see Fig. 10 and Fig. S6). This will be discussed specifically in Section 4.1.

After ANOVA testing the consistency of MODIS and VIIRS product quality (see Table S1), the RI inconsistency of B2 and B3 were more significant ($P < 0.05$), while the other biome types showed strong consistency. For StdLAI, all biome types showed significant consistency. By comparison of RI and StdLAI, we found that MODIS and VIIRS showed more significant consistency on StdLAI than RI.

Fig. 2 shows biome-specific seasonal variations of LAI and RI based on the BELMANIP sites located in the Northern Hemisphere. During the MODIS-VIIRS overlapping period (2013–2019), the MODIS LAI seasonality (large LAI in summer and low LAI in winter) was generally consistent with VIIRS for all seven biome types. It was worth noting that most biome types showed a reduced coverage of high-quality retrievals in low LAI values. Thus the RI also showed a clear seasonality. Most biome types had an increased RI in summer and a relatively reduced RI in winter (due to snow and polar night), but DBF (B6) had an increased RI in spring and fall and a relatively reduced RI in the summer and winter. From Fig. 2 (b) and (d), we can see that forest biomes (Biome 5–7) had larger LAI values and broader range than non-forest biomes (Biome 1–4). Except for EBF, whose interannual LAI values fluctuated around 4.5, forest biomes showed much clearer seasonality.

3.2. Inter-annual stability analysis of LAI and its product quality

The interannual stability analysis of annual averaged LAI, RI, and StdLAI extracted from the MODIS and VIIRS products are showed in Fig. 3. Comparing the LAI and its product qualities, we can observe that, for most cases, the interannual variations (denoted by CV values) of RI and StdLAI were both smaller than those of LAI. RI shows less volatility

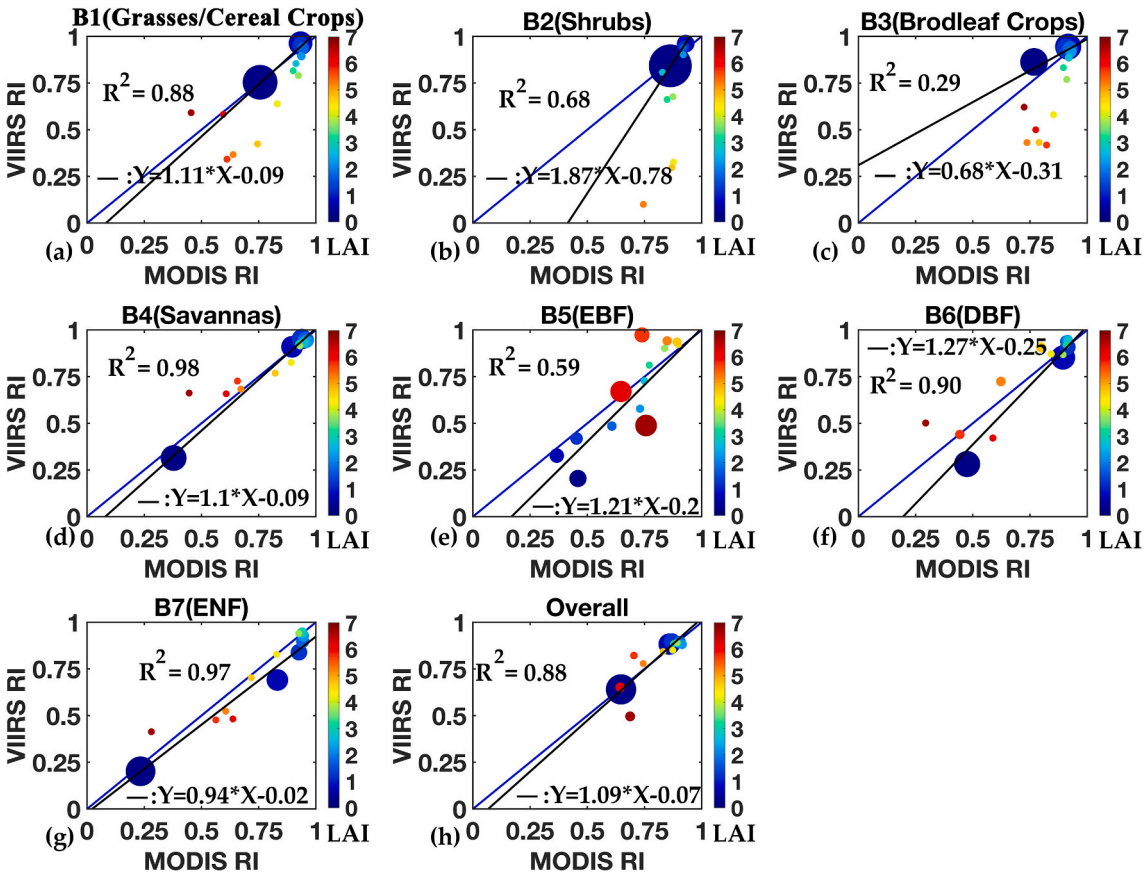

Fig. 1. Comparisons between annual averaged Retrieval Index (RI, the first selected product quality metric) of MOD15A2H and VNP15A2H for each biome. Colors of dotted symbols correspond to LAI magnitudes ranging from near 0 to 7 and the radius of dotted symbols means the proportion of pixels in that LAI range (The higher the percentage, the radius of the circle and the circle itself are larger.). Blue and black lines are the diagonals and linear fit lines, respectively. The seven biome types are: grasses and cereal crops (B1), shrubs (B2), broadleaf crops (B3), savannas (B4), evergreen broadleaf forest (EBF, B5), deciduous broadleaf forest (DBF, B6), and evergreen needleleaf forest (ENF, B7). Overall represents averages of all 7 biome types. (For interpretation of the references to color in this figure legend, the reader is referred to the web version of this article.)

compared with StdLAI for all biome types. EBF (B5) is distinct from the other biome types, showing relatively large interannual volatility for both LAI, RI, and StdLAI. The results indicate that there were more significant interannual changes in LAI magnitudes, and its product quality metrics were more stable. StdLAI showed larger fluctuations than RI due to changes in LAIs, which is explained in Section 4.1. Compared to MODIS, VIIRS was more stable (smaller CV), both in terms of LAI magnitude and its product quality metrics, which may be caused by the different study periods used for MODIS (2001–2019) and VIIRS (2013–2019). MODIS showed clearly increasing or decreasing trends in LAI magnitude and product quality metrics for some biome types. Based on the MK test, during 2001–2019, grasses and cereal crops (B1: 3.5%/decade), broadleaf crops (B3: 4.1%/decade), savannas (B4: 4.5%/decade), EBF (B5: 4.0%/decade), DBF (B6: 13.8%/decade), and ENF (B7: 10.5%/decade) showed extremely significant increasing trends for LAI. When we mixed biome types, we found a highly significant 4.5%/decade increasing trend for LAI. These biome types also showed significant trends for RI (B4: 0.9%/decade, B5: −3.3%/decade, B6: 0.2%/decade, and B7: 2.6%/decade) and StdLAI (B1: 1.7%/decade, B3: 0.1%/decade, B5: 0.2%/decade, and B6: 6.1%/decade). However, when we mixed all biome types, there was no significant trend for either RI or StdLAI, which means that theoretically there was no significant change in the quality of MODIS LAI. This result proves the effectiveness of the re-calibration and correction efforts from the MODIS science team in the context of sensor degradation (Lyapustin et al., 2014), and the goodness and robustness of the LAI retrieval algorithm.

Fig. 4 shows the percentage comparison of three different change types for MODIS LAI, RI, and StdLAI from 2001 to 2019. Compared with LAI, fewer pixels showed significant trends in their product quality metrics. Around 63% ~ 94% (depending on biome types) pixels showed a non-significant LAI trend and these numbers increased to 80% ~ 97% for RI and 76% ~ 96% for StdLAI. Many pixels show a significant increasing trend due to the high correlation between StdLAI and LAI (discussed in Section 4.1). Compared with StdLAI, the percentage of significant increase in RI (less by 0.75% - 17.3%) was lower for all biome types except shrubs. There was a larger percentage of pixels showing an increasing rather than decreasing trend in RI for all biomes except EBF, which indicates that the overall reliability of LAI is slightly improving. In addition, very few pixels (< 1%) with clear LAI trends show significantly decreasing trends of RI and significantly increasing trends of StdLAI for all seven biome types.

3.3. Spatial patterns of product quality in inter-annual stability

LAI product quality and its magnitude are related to biome type, geographical location, topography, and local climate conditions, etc. Therefore, we mapped the CV values of LAI, RI and StdLAI from the MODIS and VIIRS products over all over the world to check their interannual stability by downscaling method (500 m - 5 km). Fig. 5a-2 and b-2 show a lighter color for the two RI figures, which indicated that the RI was less variable than LAI and StdLAI. This is even more pronounced in Fig. 5c and d that the CVs of RI is smaller than that of LAI and StdLAI. The similar values and strong spatial agreement between the CV of LAI and StdLAI for both MODIS and VIIRS are shown in Fig. 5.

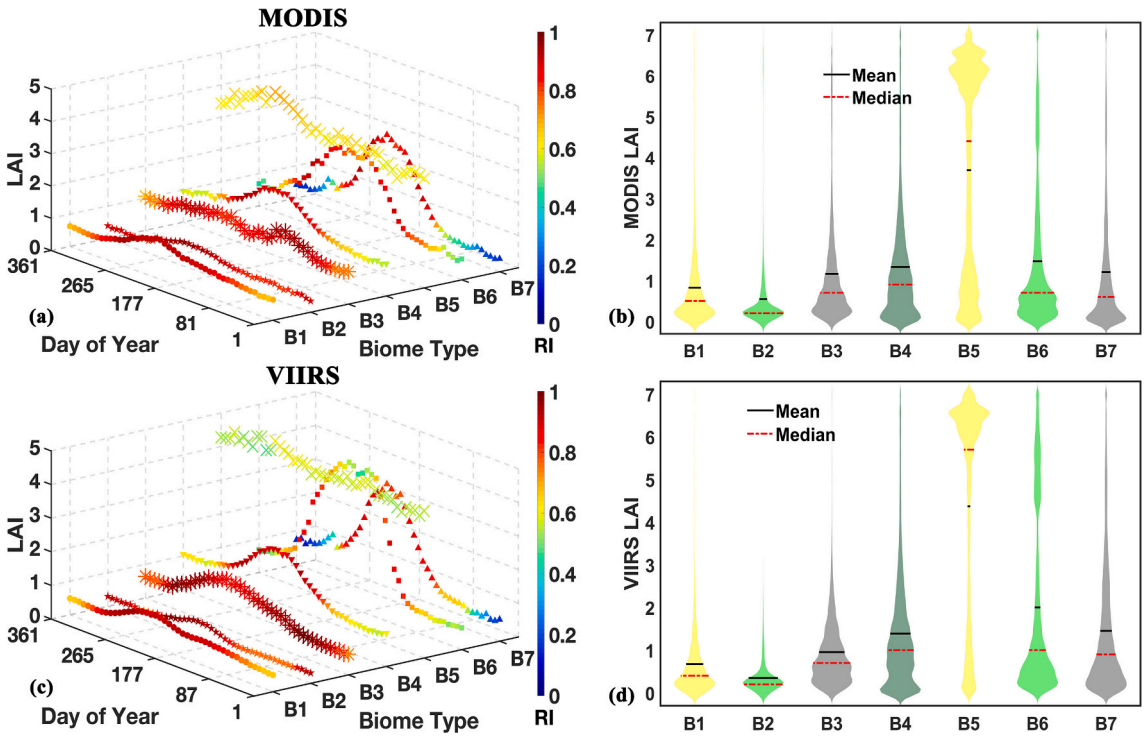

Fig. 2. The 7-year averaged (2013–2019) Retrieval Index (RI, indicated by different colors) and the LAI as a function of biome type and day of the year for MODIS (a) and VIIRS (c). Only the BELMANIP sites located in the Northern Hemisphere were used. Panels (b) and (d) are the approximate range of LAI in different biome types for MODIS and VIIRS, respectively.

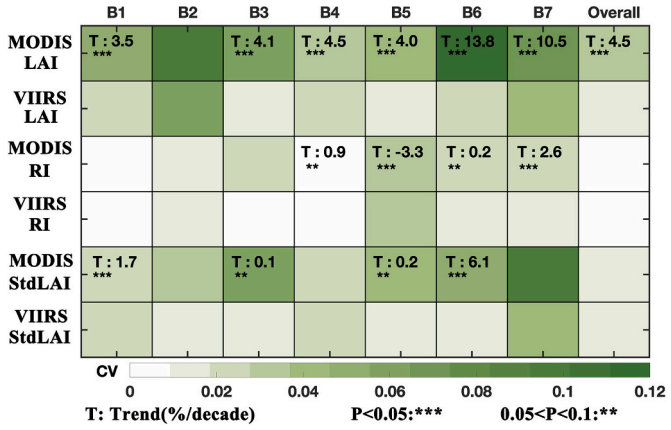

Fig. 3. Interannual stability analysis (trend and Coefficient of Variation (CV)) of annual averaged biome-specific LAI, RI, and StdLAI over 2001–2019 for MODIS and 2013–2019 for VIIRS. The color shade relates to the CV value. Trend statistics are based on Mann-Kendall test ($P < 0.05$: extremely significant change, $0.05 < P < 0.1$: weakly significant change); the trend detection was only calculated for MODIS LAI and uncertainty metrics (i.e. rows 1, 3, and 5).

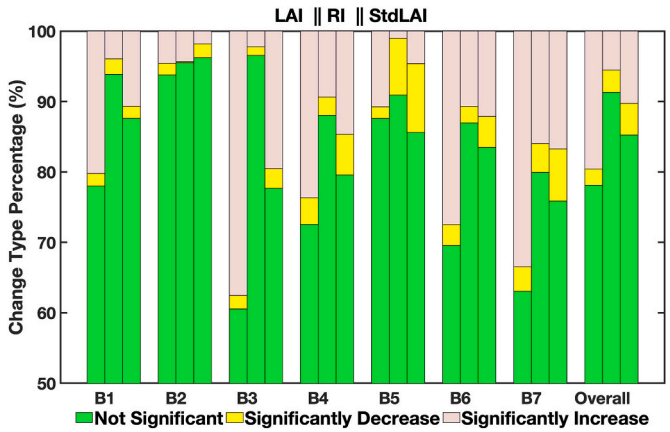

Fig. 4. Percentage of three different change types (not significant change, significant decrease, and significant increase) of MODIS LAI, RI, and StdLAI from 2001 to 2019. The "statistically significant" is tested by the Mann-Kendall test with $p \leq 0.05$. The three bars for each biome type are LAI, RI, and StdLAI from left to right, respectively. The "Overall" means the mixing-up of all seven biomes.

Additionally, we can also observe that the spatial distribution of the CV was highly consistent between MODIS and VIIRS, both for the LAI magnitude and its product qualities. Inter-annual variations of LAI and StdLAI vary with latitude, generally showing higher CVs at higher latitudes than at lower latitudes (except in the Arctic). The CV peaks of RI in tropics can be explained by the larger inter-annual variations of atmosphere conditions (rainy or cloudy).

In Fig. 6 we mapped the trends of MODIS LAI and its product qualities all over the world. Compared to RI, StdLAI shows fewer white pixels, indicating that the product quality did not show a significant trend, indicating that StdLAI has a more significant trend. Same as in Fig. 5, LAI and StdLAI show obvious spatial consistency (due to the correlation with LAI, discussed in Section 4.1). We also notice some scattered colored pixels which cannot support us to draw a consistent conclusion of decreasing or increasing trend. LAI in the mid-latitude and high-latitude vegetation zones of the Northern Hemisphere shows a more consistent increasing trend, which is consistent with published trend studies.

We also mapped the CV values (Fig. S4) of LAI, RI, and StdLAI from the MODIS and VIIRS products and the trends (Fig. S5) of MODIS LAI, RI, and StdLAI over seven single-biome-dominated tiles. The results showed the variability of RI was less variable than LAI and StdLAI in all

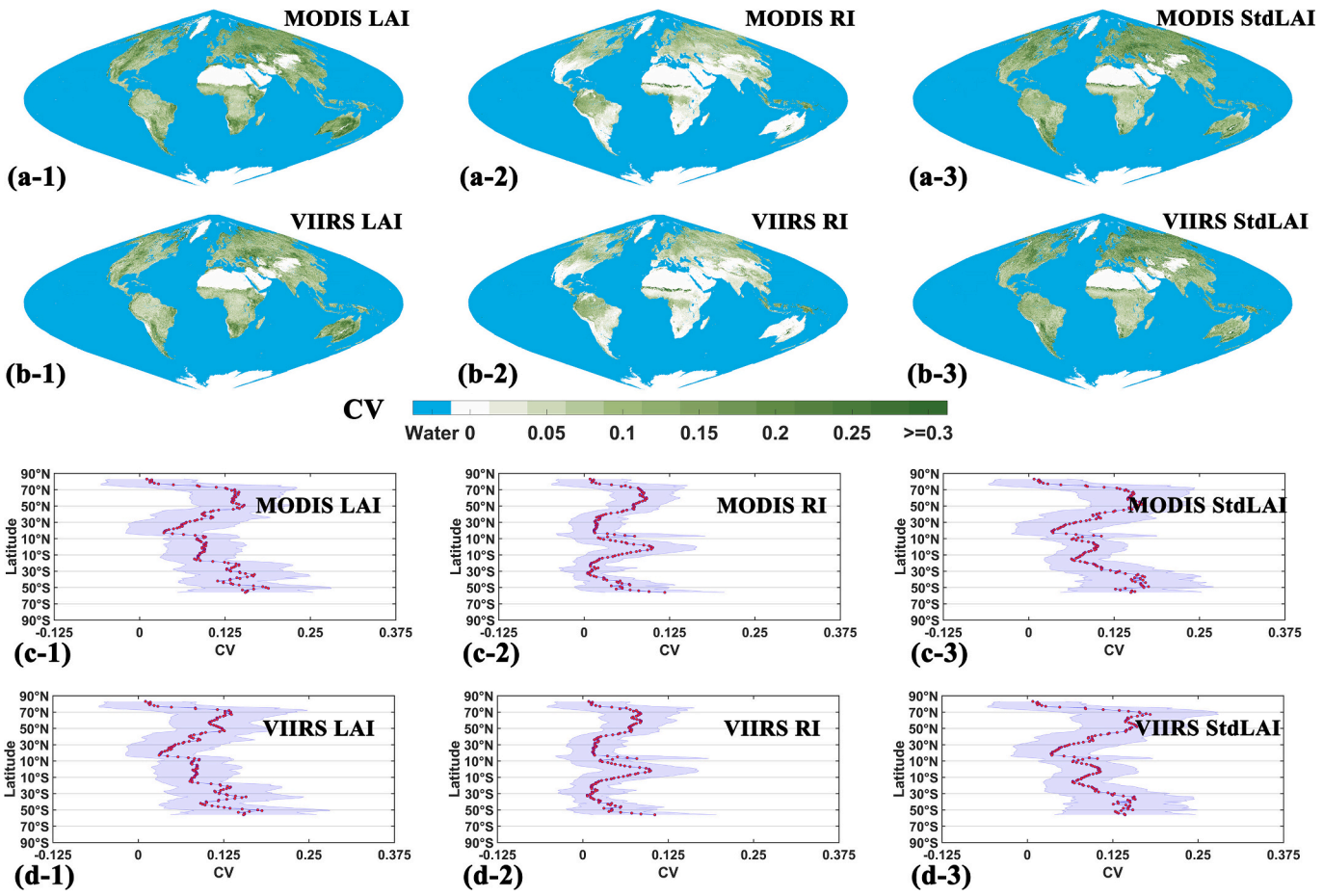

Fig. 5. Spatial distribution of CVs extracted from MODIS and VIIRS inter-annual LAI magnitude and its quality metrics. A larger CV value corresponds to larger inter-annual variations and less stability. LAI, RI, and StdLAI for two LAI products were plotted globally using the nearest sampling method (from 500 m to 5 km). Panel (a) and (c) are MODIS from 2001 to 2019 and panel (b) and (d) are VIIRS from 2013 to 2019, respectively. Panels (c) and (d) represent latitudinal transects (1° interval) of CV values for LAI, RI, and StdLAI. Red dots and shadows represent the mean values and standard deviations of CV of the 1° latitude zone. The three columns from left to right are LAI, RI, and StdLAI, respectively. (For interpretation of the references to color in this figure legend, the reader is referred to the web version of this article.)

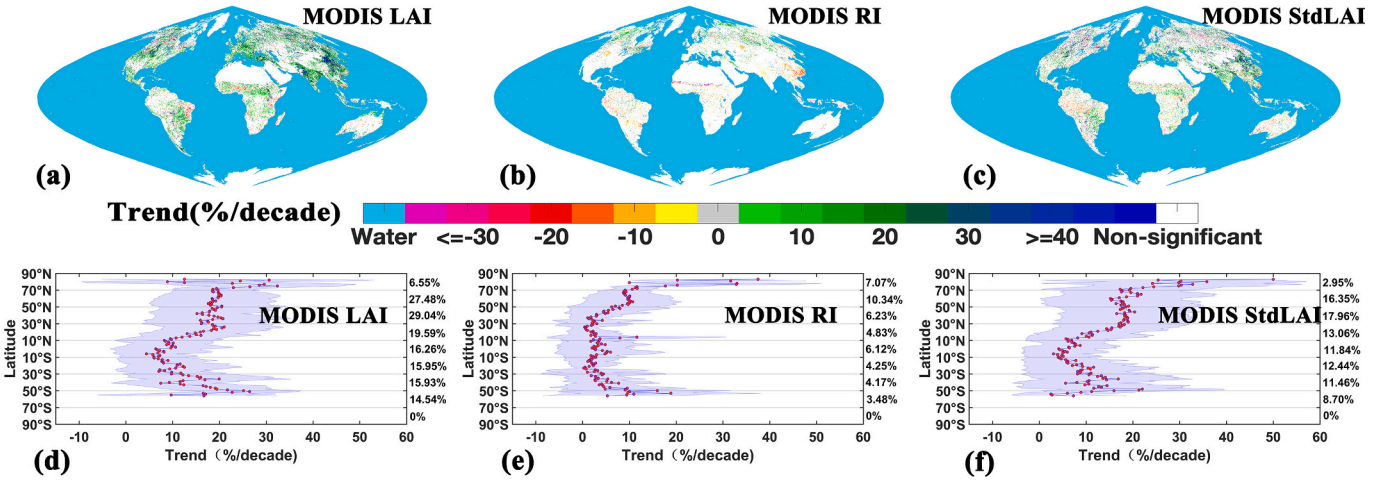

Fig. 6. Spatial distribution of the trends extracted from MODIS inter-annual LAI magnitude and its quality metrics. Same as Fig. 5 but for MODIS trends during the period 2001–2019. The white-colored pixels show no significant trend based on the Mann-Kendall test ($p \leq 0.05$). Panels (d), (e), and (f) represent latitudinal transects (1° interval) of trend values. Red dots and shadows represent the mean values and standard deviations of trend of the 1° latitude zone. The values on the right side of the panel (d), (e), and (f) indicate the proportion of pixels showing a significant trend within each 20° latitude band. (For interpretation of the references to color in this figure legend, the reader is referred to the web version of this article.)

biome types except h11v09 (B5). LAI and StdLAI showed obvious spatial consistency for CV values and trends. Additionally, there was a clear decreasing trend in product qualities (RI increases and StdLAI decreases) for a large proportion of pixels in biome 4, 6, and 7 over the study period.

3.4. Revisiting the "Greening Asia"

As reported by recent remote sensing-based studies, Asia, especially over China and India, has witnessed a clear greening trend. Here we revisit the "Greening Asia" hypothesis to check its credibility in the view of product quality. Inter-annual CV values and trends of both LAI and its product qualities are plotted in Figs. 7, 8 and 9 for two periods (2001–2019 for MODIS and 2013–2019 for VIIRS). Comparing to RI, LAI and StdLAI showed greater volatility (greater CV value), and LAI and StdLAI had more pixels with significant trends for MODIS.

During the MODIS record period (2001–2019), most parts of China and India witnessed a clear pattern of greening (green to blue-colored pixels in Fig. 9a) which is consistent with previous studies (Chen et al., 2019; Zhang et al., 2017; Zhu et al., 2016); in contrast, Southeast Asia and Siberia showed some browning trends (>30%/decade decreases of LAI). Statistically, 33.09% of the vegetated area has been greening and only 1.73% was browning in the whole Asia region from 2001 to 2019. Moreover, we noticed a 15–20%/decade decreasing trend of RI over 3.62% pixels of the whole region (e.g. Southeast China in Fig. 9b), which means that the main algorithm retrieval rate has been decreasing over these regions. We also noted that both LAI and StdLAI passed the M-K test, with a trend of 7.72%/decade for LAI and 2.09%/decade for StdLAI, while RI showed no significant change trend. Comparing Fig. 9a, b, and c, we found that pixels with clear LAI trends did not show significantly decreasing trends of RI or significantly increasing trends of StdLAI, which indicates that the greening or browning phenomenon was not caused artificially by the change of product quality. In Fig. 9d, LAI and StdLAI showed consistent rising trends while RI did not show an obvious trend. These results make the reports of "Greening Asia" more credible by eliminating the possibility of artificial trends caused by changes in LAI product quality.

4. Discussion

4.1. Product quality varies with LAI magnitude

Based on the uncertainty theory embedded in the retrieval algorithm, the retrieval accuracy is expected to vary with both biome type and LAI magnitude. Here we discuss how the changes in LAI affect product qualities. Comparing Fig. 10 and Fig. S6, it can be found that the retrievals of the three algorithm paths of MODIS and VIIRS were consistent, in agreement with what was reported by Yan et al. (Yan et al., 2018). As expected, the algorithms used were main-without-saturation and backup algorithms at low LAI values. However, as LAI increased above a threshold (about 3.5), more main-with-saturation appeared. We also found that the StdLAIs were small at low or high LAI and reached their maximum at medium LAI values (about 4–5). This situation conformed to the retrieval algorithm, that is, when the LAI is close to 0, there is a lot of non-vegetation information in the observed reflectance, which does not meet the conditions of the main algorithm and the back-

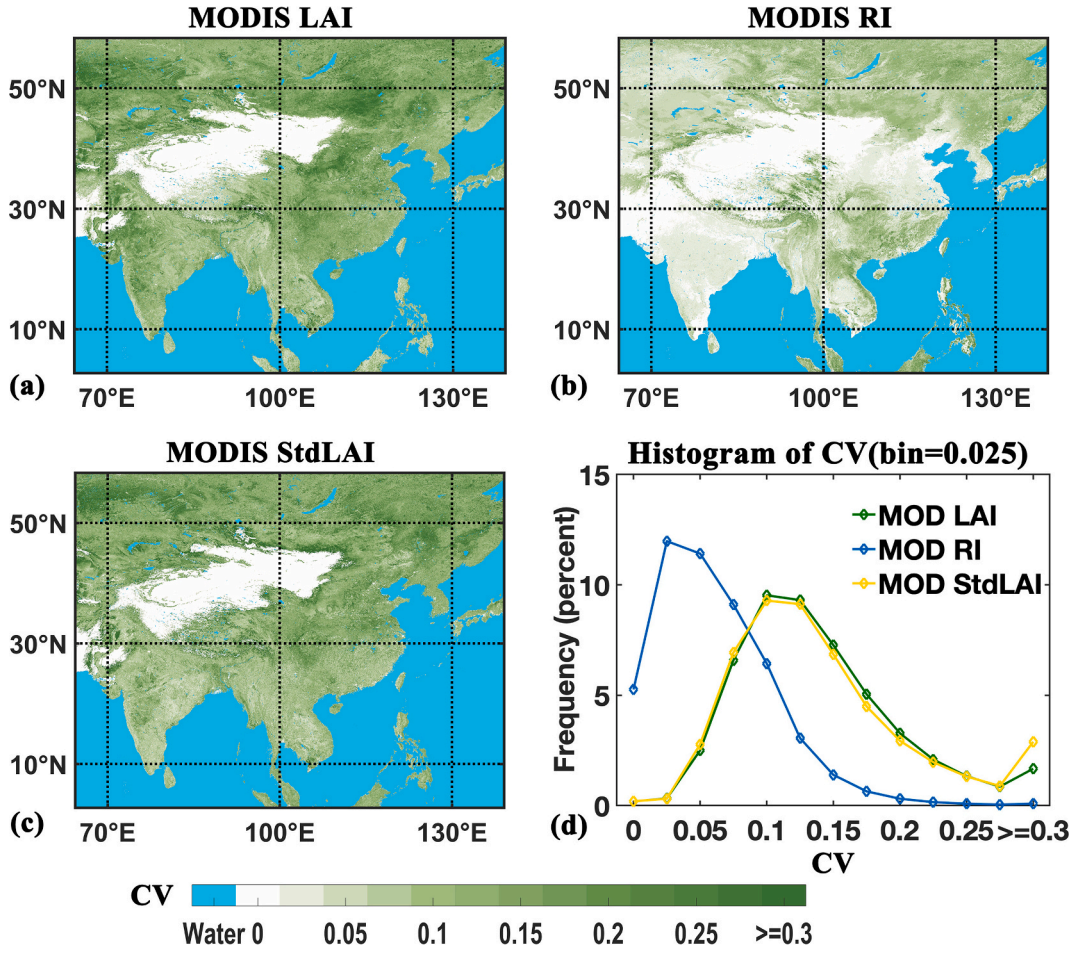

Fig. 7. Maps of Coefficient of Variation (CV) of interannual MODIS LAI and its product quality metrics (RI and StdLAI) from 2001 to 2019 in Asia (a-c). Histograms of these CV are shown in panel (d).

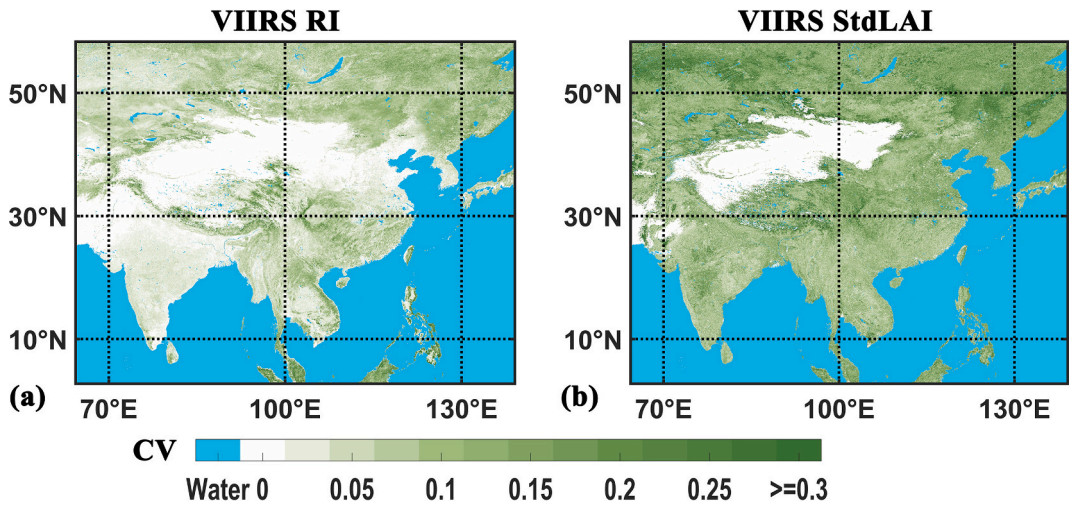

Fig. 8. Same as Fig. 7 but for VIIRS. Maps of Coefficient of Variation (CV) of interannual VIIRS product quality metrics (RI and StdLAI) from 2013 to 2019 in Asia (a-b).

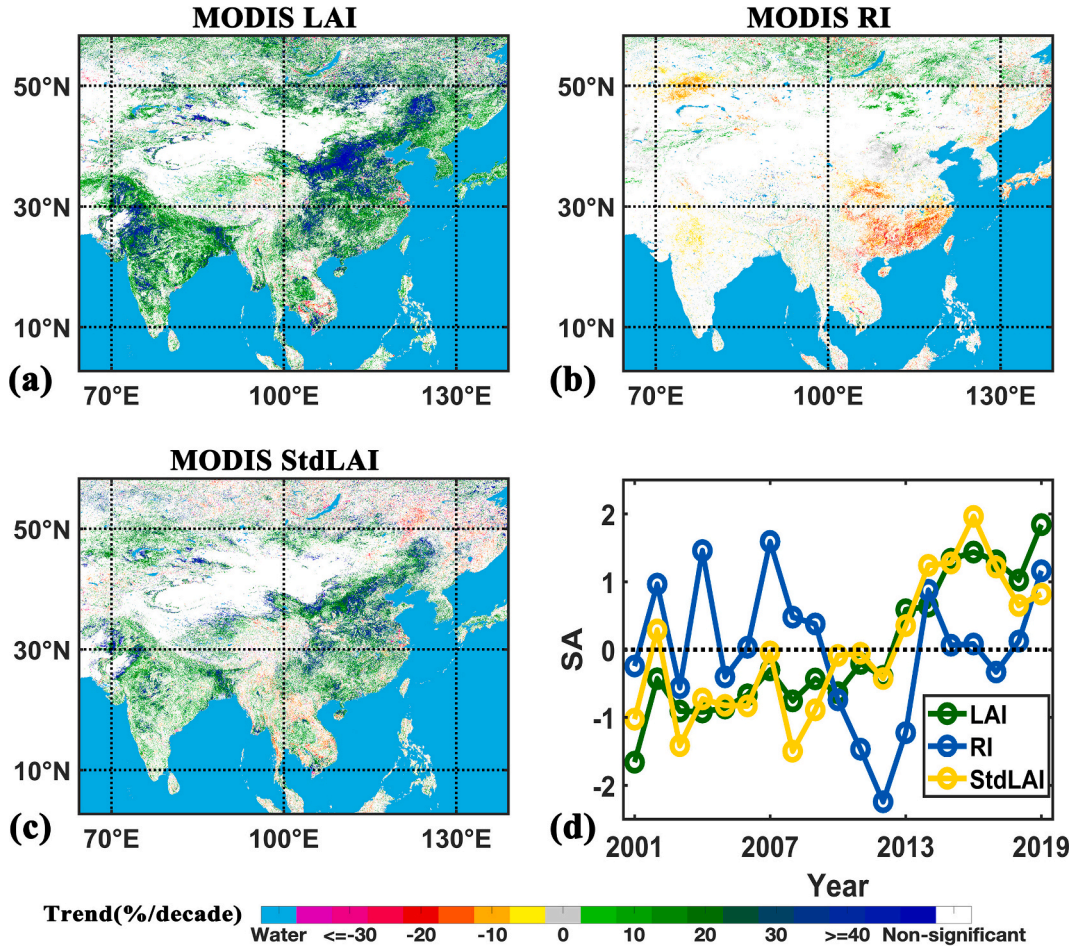

Fig. 9. Panel (a), (b), and (c) are the same as in Fig. 7 but for change trends of MODIS LAI and its product quality metrics (RI and StdLAI) during 2001 to 2019) in Asia. The white-colored pixels show no significant trend based on the Mann-Kendall test ($p \leq 0.05$). Panel (d) shows the inter-annual variation of the standard anomaly (SA) across the selected Asia region over 19 years.

up algorithm (i.e. the NDVI-LAI relationship) is triggered and no StdLAI is reported (StdLAI is only generated when the main algorithm is used). When the LAI is relatively small (< 4), there is no saturation and the LAI candidates are sparsely distributed in the NIR-Red retrieval space, which results in low standard deviation of these candidates (StdLAI) (Yan et al., 2018). As the LAI increases, the LAI candidates become denser, thus in the reflectance error ellipse, the standard deviation increases and finally triggers the main-with-saturation algorithm path. This explains the consistency between LAI and StdLAI changes shown in the above results. The StdLAI vs. LAI curve breaks is employed when it should level off is

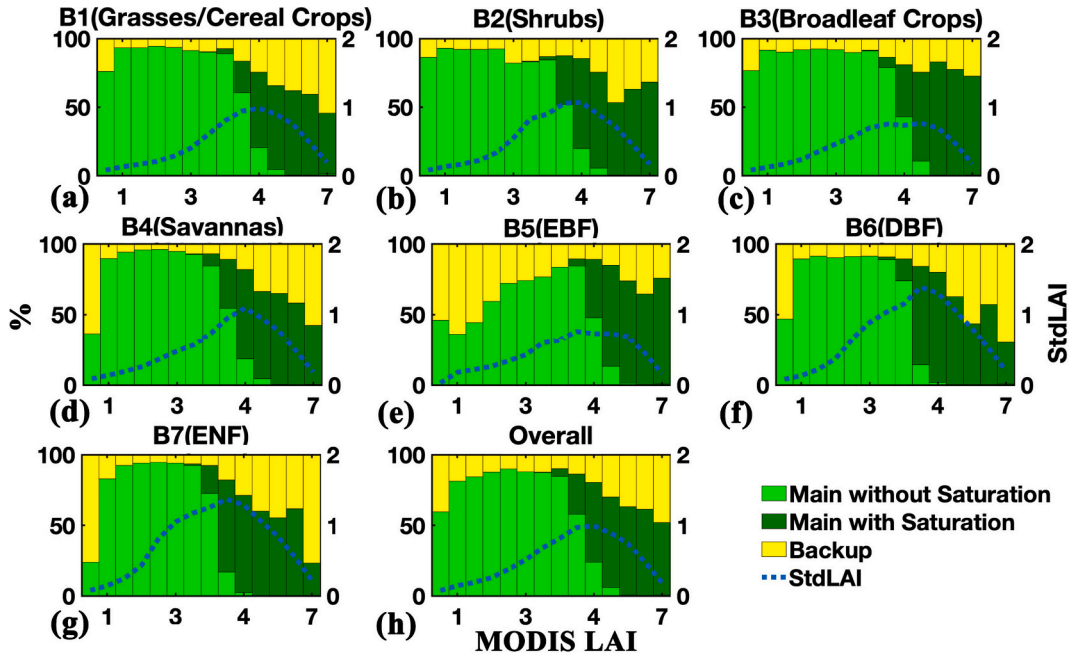

Fig. 10. Retrieval rates of three kinds of algorithm paths (two kinds of the main algorithm and one back-up algorithm) and the values of annual averaged StdLAI as a function of different LAI magnitudes for MODIS product.

that a regularization technique, which due to reduce the sensitivity of the reflectance to LAI retrievals at high LAI values (Knyazikhin, 1999). For this reason, StdLAI cannot objectively reflect the retrieval accuracy when LAI is large.

From the perspective of these two LAI products, the change of LAI magnitude did affect the product quality metrics for all biome types. The seasonality of LAI caused seasonality of RI and StdLAI, resulting in differences in product accuracy at different times of the year (Fig. 2). Theoretically, the trend of the LAI time-series also affects the change of product quality. While the fact is that whether the product quality metrics decreased or increased depended on the biome type, the extent of changes in LAI, and the trend in LAI. Therefore, the interannual variation in product quality could be ignored when the LAI changed slightly, but when the LAI has a significant increasing or decreasing trend, we will need to pay attention to product accuracy.

4.2. *Product quality varies with Atmospheric conditions*

Except for the theoretical uncertainty in the algorithm, the input reflectance uncertainty (mainly caused by atmospheric correction) can affect product quality, including sensor degradation and cloud/aerosol variability. Other than this, changes in atmospheric conditions will also have an effect on LAI retrieval accuracy. Thus, we need to exclude this effect to better analyze the effect of sensor degradation on the LAI quality. Here we tested the hypothesis that the change in product quality is due to changes in cloud/aerosol, rather than to uncertainty in the algorithm itself, BRF uncertainty, and sensor degradation. Therefore, we analyzed the relationship between LAI product quality metrics and

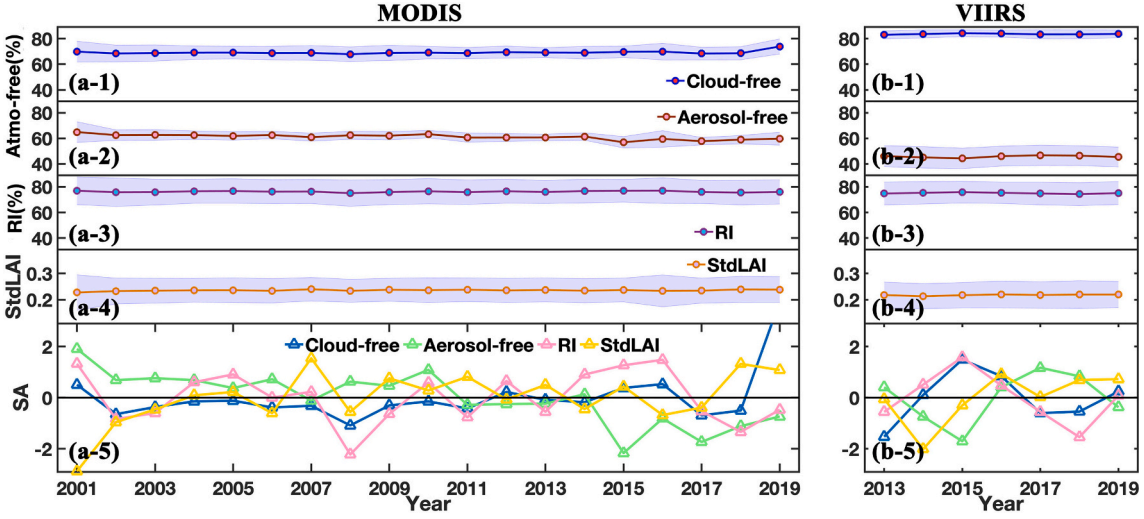

Fig. 11. Interannual variation of the percentage of cloud-free/aerosol-free pixels and LAI product quality metrics (RI and StdLAI) for MODIS (left) and VIIRS (right). a-1, b-1 and a-2, b-2 show the annual average percentage of cloud-free and aerosol-free pixels, respectively. a-3, b-3 and a-4, b-4 show the annual average RI and StdLAI, respectively. Dots are the mean values and shadows indicate the standard deviation. a-5 and b-5 show the standardized anomaly (SA) of the two product quality metrics and of the two atmospheric conditions. The atmospheric conditions of the two LAI products investigated in this study are given in Table S2.

atmospheric conditions. Since these BELMANIP sites are located on the plains (rather than in mountain areas), the percentage of cloud-free (70% - 80%) and aerosol-free (50%–60%) pixels at the global scale were overestimated. From Fig. 11, we found that the interannual atmospheric conditions remained stable during both the MODIS and VIIRS periods. However, compared with MODIS, VIIRS overestimated the percentage of cloud-free and underestimated the percentage of aerosol-free pixels, which may be caused by the different atmospheric flags (see Table S2) and transit time. Since MODIS has more bands than VIIRS, and other sensors onboard the same satellite (e.g. MISR) can detect atmospheric conditions, the MODIS product should have better atmospheric monitoring accuracy than VIIRS. Moreover, from Fig. 12, we found that the RI of MODIS was more affected by clouds, while VIIRS was more affected by aerosols. For MODIS (VIIRS), the R^2 between RI and the percentage of no-cloud and no-aerosol were 0.22 (0.87) and 0.77 (0.69), respectively. We also found that the effect of cloud/aerosol on RI was greater than on StdLAI.

From the above analysis, the atmospheric conditions that affected the quality of the LAI products, such as clouds and aerosols, did not show obvious interannual changes. Therefore, we can ignore the impact of atmospheric conditions on the changes in product quality. However, the correlation between atmospheric conditions and LAI product quality means that to account for future variations in cloud and aerosol fluctuations, the quality of the LAI products will need to be re-evaluated.

4.3. Limitation of this study

It is worth noting that there are some limitations with the way we investigate the algorithm performance stability. Firstly, since that the short operational period of VIIRS (2013–2019) was not statistically sufficient to support trend analysis, the trend detection was only calculated for MODIS product. Secondly, this study lacks the results of performance analysis for different algorithm paths (i.e., main algorithms and backup algorithms). In future studies, we will test the robustness of each retrieval algorithm path, which will provide a more comprehensive evaluation of the operational algorithm.

The two product quality metrics portray the theoretical uncertainty of the algorithm, which is different from the absolute uncertainty of the product obtained from ground-based validation (De Kauwe et al., 2011; Yan et al., 2016b), and the readers should be aware. Due to the lack of independent high-quality long-term in situ dataset, we did not do a traditional product validation, and thus this study cannot give absolute uncertainties of the products. Although we cannot answer how the magnitude and variation of the absolute uncertainty of the products over 20 years, this study can demonstrate the stability of the retrieval algorithm and indirectly illustrate the reliability of the products. Therefore, the study is necessary for the theoretical purpose in comparison to ground-based validation and is useful for algorithm improvement. Moreover, this kind of indirect product evaluation does not depend on the uncertainty of ground measurements and thus is more objective on a global scale.

5. Concluding remarks

LAI has been derived from MODIS observations since 2000 and the VIIRS LAI has been generated from 2012 based on the same retrieval strategy of MODIS to ensure the continuity of these ESDRs. The MODIS and VIIRS LAI products are widely used for many long-term series trend analyses, such as for monitoring changes in global greening trends. The reliability of these studies depends on the performance stability of the LAI retrieval algorithm over time changing, for which detailed research has been missing to date. In addition, there is an urgent need to answer whether the configuration of the LAI retrieval algorithm is still applicable to the uncertainty of the current MODIS BRFs. The research is based on the assumption that there are trends and clear inter-annual variations in LAI magnitudes for long time series, however the product

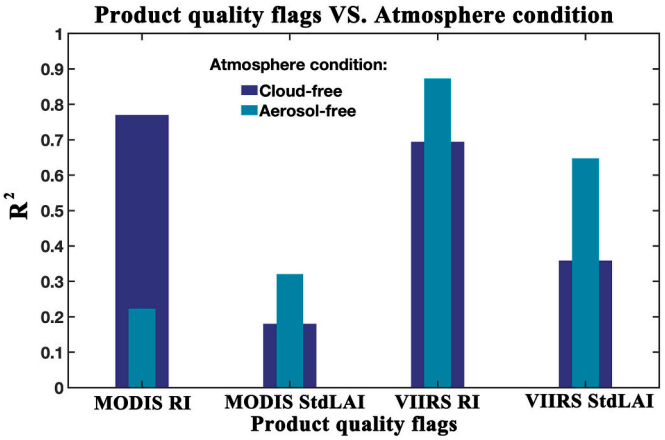

Fig. 12. Correlation between product quality metrics (RI and StdLAI) and atmospheric conditions (cloud-free and aerosol-free) in two time-series (2001–2019 for MODIS and 2013–2019 for VIIRS).

quality should keep consistency which results in much stabler quality metrics (i.e. StdLAI and RI). This paper presented an analysis of the interannual stability and trend detection for both LAI magnitude and product quality during MODIS (2001–2019) and VIIRS (2013–2019) data acquisition periods to test this hypothesis. Compared to direct ground-based validation, such theoretical studies are useful for algorithm improvement and are more objective on global scale product analysis. The results showed that the LAI values had the largest interannual variation, followed by StdLAI (due to significant positive correlation with the LAI), while RI was much more stable during these years for both MODIS and VIIRS. It also can be noticed that MODIS showed a significant trend in LAI but did not show a clear trend in its product qualities (combined analysis of RI and StdLAI) from 2001 to 2019. We conclude that the performance stability of LAI retrieval algorithm is sufficient to support trend-related studies published thus far. We also found that VIIRS has performed considerably similarly to MODIS through both temporal and spatial time-series stability analysis (R^2 was 0.88 for RI and 0.99 for StdLAI). For different biome types, product quality metrics varied seasonally, following LAI, thus there was a certain relationship between product qualities and its magnitude. Moreover, the results also indicate that small interannual variations in atmospheric conditions did not result in large changes in product qualities. A specific study showed that the “Greening Asia” had a trend of 7.72%/decade for LAI and a smaller trend (2.09%/decade) for StdLAI (high correlation between StdLAI and LAI), while the RI did not show a clear trend, which confirms previous reports. Overall, it is worth noting that both MODIS and VIIRS LAI products maintained a relatively stable performance of retrieval algorithm during their corresponding records and they show a high consistency in both LAI magnitudes and product quality levels. This illustrates that, the uncertainty of existing BRF product is still compatible with the configuration of algorithm and indirectly imbues confidence in continuing the long-term MODIS data record through VIIRS products.

Declaration of Competing Interest

The authors declare that they have no known competing financial interests or personal relationships that could have appeared to influence the work reported in this paper.

Acknowledgments

This work was supported by the National Natural Science Foundation of China (41901298, 42090013, 42001303), the open fund of State Key Laboratory of Remote Sensing Science (OFSLRSS201924), and the

Fundamental Research Funds for the Central Universities (2652018031). We acknowledge the help from the VIIRS & MODIS science team members.

Appendix A. Supplementary data

Supplementary data to this article can be found online at https://doi.org/10.1016/j.rse.2021.112438.

References

Abdi, H., 2010. Coefficient of variation. Encyclopedia Res. Design 1, 169–171.

Baret, F., Morissette, J.T., Fernandes, R.A., Champeaux, J.L., Myneni, R.B., Chen, J., Plummer, S., Weiss, M., Bacour, C., Garrigues, S., Nickeson, J.E., 2006. Evaluation of the representativeness of networks of sites for the global validation and intercomparison of land biophysical products: proposition of the CEOS-BELMANIP. IEEE Trans. Geosci. Remote Sens. 44, 1794–1803.

Bartholome, E., Belward, A.S., 2005. GLC2000: a new approach to global land cover mapping from earth observation data. Int. J. Remote Sens. 26, 1959–1977.

Chakroun, H., Mouillot, F., Nasr, Z., Nouri, M., Ennajah, A., Ourcival, J., 2014. Performance of LAI-MODIS and the influence on drought simulation in a Mediterranean forest. Ecohydrology 7, 1014–1028.

Chen, L., Dirmeyer, P.A., 2016. Adapting observationally based metrics of biogeophysical feedbacks from land cover/land use change to climate modeling. Environ. Res. Lett. 11, 034002.

Chen, C., Park, T., Wang, X., Piao, S., Xu, B., Chaturvedi, R.K., Fuchs, R., Brovkin, V., Ciais, P., Fensholt, R., Tommervik, H., Bala, G., Zhu, Z., Nemani, R.R., Myneni, R.B., 2019. China and India lead in greening of the world through land-use management. Nat. Sustain. 2, 122–129.

Claverie, M., Vermote, E.F., Weiss, M., Baret, F., Hagolle, O., Demarez, V., 2013. Validation of coarse spatial resolution LAI and FAPAR time series over cropland in Southwest France. Remote Sens. Environ. 139, 216–230.

De Kauwe, M.G., Disney, M., Quaife, T., Lewis, P., Williams, M., 2011. An assessment of the MODIS collection 5 leaf area index product for a region of mixed coniferous forest. Remote Sens. Environ. 115, 767–780.

Dhorde, A., Patel, N., 2016. Spatio-temporal variation in terminal drought over western India using dryness index derived from long-term MODIS data. Ecol. Inform. 32, 28–38.

Fang, H., Wei, S., Liang, S., 2012. Validation of MODIS and CYCLOPES LAI products using global field measurement data. Remote Sens. Environ. 119, 43–54.

Fang, H., Jiang, C., Li, W., Wei, S., Baret, F., Chen, J.M., Garcia-Haro, J., Liang, S., Liu, R., Myneni, R.B., Pinty, B., Xiao, Z., Zhu, Z., 2013. Characterization and intercomparison of global moderate resolution leaf area index (LAI) products: analysis of climatologies and theoretical uncertainties. J. Geophys. Res. Biogeosci. 118, 529–548. https://doi.org/10.1002/jgrg.20051.

Fang, H., Baret, F., Plummer, S., Schaepman-Strub, G., 2019. An overview of global leaf area index (LAI): methods, products, validation, and applications. Rev. Geophys. 57, 739–799.

Fuster, B., Sánchez-Zapero, J., Camacho, F., García-Santos, V., Verger, A., Lacaze, R., Weiss, M., Baret, F., Smets, B., 2020. Quality assessment of PROBA-V LAI, fAPAR and fCOVER collection 300 m products of Copernicus global land service. Remote Sens. 12, 1017.

Gocic, M., Trajkovic, S., 2013. Analysis of changes in meteorological variables using Mann-Kendall and Sen's slope estimator statistical tests in Serbia. Glob. Planet. Chang. 100, 172–182.

Hill, M.J., Senarath, U., Lee, A., Zeppel, M., Nightingale, J.M., Williams, R.D.J., McVicar, T.R., 2006. Assessment of the MODIS LAI product for Australian ecosystems. Remote Sens. Environ. 101, 495–518.

Jacquemoud, S., Baret, F., Hanocq, J., 1992. Modeling spectral and bidirectional soil reflectance. Remote Sens. Environ. 41, 123–132.

Justice, C.O., Román, M.O., Csiszar, I., Vermote, E.F., Wolfe, R.E., Hook, S.J., Friedl, M., Wang, Z., Schaaf, C.B., Miura, T., 2013. Land and cryosphere products from Suomi NPP VIIRS: overview and status. J. Geophys. Res.-Atmos. 118, 9753–9765.

Kala, J., Decker, M., Exbrayat, J.-F., Pitman, A.J., Carouge, C., Evans, J.P., Abramowitz, G., Mocko, D., 2014. Influence of leaf area index prescriptions on simulations of heat, moisture, and carbon fluxes. J. Hydrometeorol. 15, 489–503.

Knyazikhin, Y., 1999. MODIS Leaf Area Index (LAI) and Fraction of Photosynthetically Active Radiation Absorbed by Vegetation (FPAR) Product (MOD 15) Algorithm Theoretical Basis Document. https://modis.gsfc.nasa.gov/data/atbd/atbd_mod15.pdf.

Knyazikhin, Y., Myneni, R., 2018. VIIRS Leaf Area Index (LAI) and Fraction of Photosynthetically Active Radiation Absorbed by Vegetation (FPAR) User Guide.

Knyazikhin, Y., Martonchik, J., Myneni, R.B., Diner, D., Running, S.W., 1998. Synergistic algorithm for estimating vegetation canopy leaf area index and fraction of absorbed photosynthetically active radiation from MODIS and MISR data. J. Geophys. Res.-Atmos. 103, 32257–32275.

Lafont, S., Zhao, Y., Calvet, J.-C., Peylin, P., Ciais, P., Maignan, F., Weiss, M., 2012. Modelling LAI, surface water and carbon fluxes at high-resolution over France: comparison of ISBA-A-gs and ORCHIDEE. Biogeosciences 9.

Liu, Y., Xiao, J., Ju, W., Zhu, G., Wu, X., Fan, W., Li, D., Zhou, Y., 2018. Satellite-derived LAI products exhibit large discrepancies and can lead to substantial uncertainty in simulated carbon and water fluxes. Remote Sens. Environ. 206, 174–188.

Lyapustin, A., Wang, Y., Xiong, X., Meister, G., Platnick, S., Levy, R., Franz, B., Korkin, S., Hilker, T., Tucker, J., Hall, F., Sellers, P., Wu, A., Angal, A., 2014. Scientific impact of MODIS C5 calibration degradation and C6+ improvements. Atmos. Measure. Tech. 7, 4353–4365.

MacBean, N., Maignan, F., Peylin, P., Bacour, C., Bréon, F.-M., Ciais, P., 2015. Using satellite data to improve the leaf phenology of a global terrestrial biosphere model. Biogeosci. Discuss. 12.

Mao, J., Shi, X., Thornton, P.E., Hoffman, F.M., Zhu, Z., Myneni, R.B., 2013. Global latitudinal-asymmetric vegetation growth trends and their driving mechanisms: 1982–2009. Remote Sens. 5, 1484–1497.

Mariano, D.A., Santos, C.A.C.D., Wardlow, B.D., Anderson, M.C., Schiltmeyer, A.V., Tadesse, T., Svoboda, M., 2018. Use of remote sensing indicators to assess effects of drought and human-induced land degradation on ecosystem health in Northeastern Brazil. Remote Sens. Environ. 213, 129–143.

Myneni, R., Park, Y., 2015. MODIS Collection 6 (C6) LAI/FPAR Product User's Guide. Feb, In.

Myneni, R.B., Hoffman, S., Knyazikhin, Y., Privette, J., Glassy, J., Tian, Y., Wang, Y., Song, X., Zhang, Y., Smith, G., 2002. Global products of vegetation leaf area and fraction absorbed PAR from year one of MODIS data. Remote Sens. Environ. 83, 214–231.

Park, T., Yan, K., Chen, C., Xu, B., Knyazikhin, Y., Myneni, R., 2017. VIIRS Leaf Area Index (LAI) and Fraction of Photosynthetically Active Radiation Absorbed by Vegetation (FPAR) Product Algorithm Theoretical Basis Document (ATBD) (NASA Technical Report).

Sellers, P., Dickinson, R.E., Randall, D., Betts, A., Hall, F., Berry, J., Collatz, G., Denning, A., Mooney, H., Nobre, C., 1997. Modeling the exchanges of energy, water, and carbon between continents and the atmosphere. Science 275, 502–509.

Serbin, S.P., Ahl, D.E., Gower, S.T., 2013. Spatial and temporal validation of the MODIS LAI and FPAR products across a boreal forest wildfire chronosequence. Remote Sens. Environ. 133, 71–84.

Skakun, S., Justice, C.O., Vermote, E., Roger, J., 2018. Transitioning from MODIS to VIIRS: an analysis of inter-consistency of NDVI data sets for agricultural monitoring. Int. J. Remote Sens. 39, 971–992.

Sulla-Menashe, D., Friedl, M.A.J.U.R., 2018. User Guide to Collection 6 MODIS Land Cover (MCD12Q1 and MCD12C1) Product. VA, USA.

Tang, X., Wang, Z., Xie, J., Liu, D., Desai, A.R., Jia, M., Dong, Z., Liu, X., Liu, B., 2013. Monitoring the seasonal and interannual variation of the carbon sequestration in a temperate deciduous forest with MODIS time series data. For. Ecol. Manag. 306, 150–160.

Wang, D., Liang, S., 2013. Improving LAI mapping by integrating MODIS and CYCLOPES LAI products using optimal interpolation. IEEE J. Select. Topics Appl. Earth Observ. Remote Sens. 7, 445–457.

Wang, D., Morton, D., Masek, J., Wu, A., Nagol, J., Xiong, X., Levy, R., Vermote, E., Wolfe, R., 2012. Impact of sensor degradation on the MODIS NDVI time series. Remote Sens. Environ. 119, 55–61.

Weiss, M., Baret, F., Block, T., Koetz, B., Burini, A., Scholze, B., Lecharpentier, P., Brockmann, C., Fernandes, R., Plummer, S., 2014. On line validation exercise (OLIVE): a web based service for the validation of medium resolution land products. Application to FAPAR products. Remote Sens. 6, 4190–4216.

Xiong, X., Esposito, J.A., Sun, J.-Q., Pan, C., Guenther, B.W., Barnes, W.L., 2001. Degradation of MODIS Optics and its Reflective Solar Bands Calibration. SPIE.

Xiong, X., Angal, A., Wu, A., Barnes, W., Salomonson, V., 2016. Terra and Aqua MODIS instrument performance. In: 2016 IEEE International Geoscience and Remote Sensing Symposium (IGARSS). IEEE, pp. 7388–7391.

Xu, B., Park, T., Yan, K., Chen, C., Zeng, Y., Song, W., Yin, G., Li, J., Liu, Q., Knyazikhin, Y., Myneni, R., 2018. Analysis of global LAI/FPAR products from VIIRS and MODIS sensors for Spatio-temporal consistency and uncertainty from 2012–2016. Forests 9.

Yan, K., Park, T., Yan, G., Chen, C., Yang, B., Liu, Z., Nemani, R., Knyazikhin, Y., Myneni, R., 2016a. Evaluation of MODIS LAI/FPAR product collection 6. Part 1: consistency and improvements. Remote Sens. 8.

Yan, K., Park, T., Yan, G., Liu, Z., Yang, B., Chen, C., Nemani, R., Knyazikhin, Y., Myneni, R., 2016b. Evaluation of MODIS LAI/FPAR product collection 6. Part 2: validation and Intercomparison. Remote Sens. 8.

Yan, K., Park, T., Chen, C., Xu, B., Song, W., Yang, B., Zeng, Y., Liu, Z., Yan, G., Knyazikhin, Y., Myneni, R.B., 2018. Generating global products of lai and fpar from snpp-viirs data: theoretical background and implementation. IEEE Trans. Geosci. Remote Sens. 56, 2119–2137.

Yang, W., Tan, B., Huang, D., Rautiainen, M., Shabanov, N.V., Wang, Y., Privette, J.L., Huemmrich, K.F., Fensholt, R., Sandholt, I., 2006. MODIS leaf area index products: from validation to algorithm improvement. IEEE Trans. Geosci. Remote Sens. 44, 1885–1898.

Zhang, Y., Song, C., Band, L.E., Sun, G., Li, J., 2017. Reanalysis of global terrestrial vegetation trends from MODIS products: Browning or greening? Remote Sens. Environ. 191, 145–155.

Zhu, Z., Piao, S., Myneni, R.B., Huang, M., Zeng, Z., Canadell, J.G., Ciais, P., Sitch, S., Friedlingstein, P., Arneth, A., Cao, C., Cheng, L., Kato, E., Koven, C., Li, Y., Lian, X., Liu, Y., Liu, R., Mao, J., Pan, Y., Peng, S., Peñuelas, J., Poulter, B., Pugh, T.A.M., Stocker, B.D., Viovy, N., Wang, X., Wang, Y., Xiao, Z., Yang, H., Zaehle, S., Zeng, N., 2016. Greening of the earth and its drivers. Nat. Clim. Chang. 6, 791–795.